

# Sirtuin-2 Activity is Required for Glioma Stem Cell Proliferation Arrest but not Necrosis Induced by Resveratrol

Salwa Sayd · Cécile Thirant · Elias A. El-Habr · Joanna Lipecka ·  
Luiz Gustavo Dubois · Alexandra Bogeas · Nadia Tahiri-Jouti ·  
Hervé Chneiweiss · Marie-Pierre Junier

Published online: 18 August 2013  
© Springer Science+Business Media New York 2013

**Abstract** Glioblastomas, the most common form of primary brain tumors, are the fourth cause of death by cancer in adults. Increasing evidences suggest that glioblastoma resistance to existing radio- and chemotherapies rely on glioblastoma stem cells (GSCs). GSCs are endowed with a unique combination of stem-like properties alike to normal neural stem cells (NSCs), and of tumor initiating properties. The natural polyphenol resveratrol is known to exert opposite actions on neural cells according to their normal or cancerous status. Here, we used resveratrol to explore the molecular mechanisms differing between GSCs and NSCs. We observed a dual action of resveratrol on GSCs: resveratrol blocked GSC proliferation up to 150  $\mu$ M and induced their necrosis at higher doses. On the opposite, resveratrol had no effect on NSC behavior. To determine the mechanisms underlying resveratrol effects, we focused our attention on the family of NAD-dependent deacetylases sirtuins (SIRT). A member of this family, SIRT1, has been repetitively shown to constitute a preferential resveratrol target, at least in normal cells. Western blot analysis

showed that SIRT1 and SIRT3 were expressed by both GSCs and NSCs whereas SIRT2 expression was restricted to GSCs. Pharmacological blockade of SIRT2 activity or down-regulation of SIRT2 expression with siRNAs counteracted the inhibitory effect of resveratrol on cell proliferation. On the contrary, inhibition of SIRT2 activity or expression did not counteract GSC necrosis observed in presence of high doses of resveratrol. Our results highlight SIRT2 as a novel target for altering GSC properties.

**Keywords** Sirtuin · Cancer stem cell ·  $\alpha$ -tubulin · Necrosis

## Introduction

Glioblastomas are the most common and malignant primary tumors of the human adult central nervous system. Despite the combination of surgery, radiotherapy and chemotherapy, the life expectancy of patients diagnosed with glioblastoma is approximately 1 year [1]. A growing body of evidence indicates that a sub-population of tumor cells endowed with stem-like and tumor-initiating properties plays key roles in the development and therapeutic resistance of glioblastomas [2–5]. The properties of these glioblastoma stem cells (GSCs) are sustained at least in part by molecular pathways previously shown to control normal embryonic and/or neural stem cell (NSC) properties, such as the Sonic hedgehog-Gli-Nanog network [6, 7]. Several studies have disclosed an association between tumor formation by GSCs and their peculiar resistance to chemotherapy and radiation treatments, as compared to other cell populations of the tumor [8]. Experiments using lineage tracing to look for the contribution of individual tumor cells to tumor formation, suggest that the replenishment of the tumor by GSCs spared by the treatment is responsible for the failure of current therapies [4]. Deciphering molecular differences between GSCs and NSCs should help to further understand the molecular pathways

---

Hervé Chneiweiss and Marie-Pierre Junier contributed equally.

---

S. Sayd · C. Thirant · E. A. El-Habr · J. Lipecka · L. G. Dubois ·  
A. Bogeas · H. Chneiweiss · M.-P. Junier  
Team Glial Plasticity, U894 Inserm, Université Paris Descartes,  
Paris, France

S. Sayd · N. Tahiri-Jouti  
Laboratory of Genetics and Molecular Pathology, Faculty of  
Medicine and Pharmacy of Casablanca, Casablanca, Morocco

H. Chneiweiss (✉) · M.-P. Junier (✉)  
U894 Team Glial Plasticity, Center of Psychiatry and Neurosciences,  
2ter rue d'Alésia, 75014 Paris, France  
e-mail: herve.chneiweiss@inserm.fr  
e-mail: marie-pierre.junier@inserm.fr

*Present Address:*  
C. Thirant  
U1009 Inserm IGR Université Paris-XI, Villejuif, France

underlying their properties, and ultimately help in controlling their behavior whilst sparing the normal nervous tissue.

Remarkably, the plant polyphenol resveratrol has been shown to exert opposite effects on normal and cancerous cells [9]. Resveratrol (3,4,5-trihydroxy-trans-stilbene) is a natural polyphenolic phytoalexin widely present in plants and enriched in red wine, peanuts and grapes [10]. This compound has received considerable attention over the last decades, first for its use in treating cardiovascular diseases, and more recently for its neuroprotective effects associated with its ability to cross the blood–brain barrier [11]. Resveratrol beneficial effects are underlined by its antioxidant and anti-inflammatory action and include activation of enzymes such as sirtuins, which regulate longevity genes preventing the deleterious effects triggered by oxidative stress [11]. A major target of resveratrol for its pro-survival function is sirtuin-1 (SIRT1), which bears an allosteric site recognized by resveratrol [12]. SIRT1-mediated p53 deacetylation prevents p53 transcriptional activity and counteracts apoptosis in response to oxidative stress and DNA damage [13]. More recently another member of the sirtuin family, SIRT2, has got much attention due to its involvement in programmed necrosis [14]. SIRT2 is also considered as a mitotic exit regulator and was reported to suppress colony formation in glioma cell lines [15]. Resveratrol effect on SIRT2 activity is however unknown. Of note, resveratrol effects on glioma cell lines depend on the cell line studied and on the compound concentration used, and range from limitation of the proliferation [16–18], and the survival of the cells [19, 20], or enhancement of their sensitivity to the DNA alkylating agent temozolomide [21, 22]. Here, we evaluated resveratrol effects on GSC cultures derived from three distinct glioblastoma biopsies and one grade III oligoastrocytoma as compared to two cultures of human NSCs derived from fetal brains, focusing on members of the sirtuin family as possible mediators of resveratrol action on GSCs.

## Materials and Methods

### Cell Culture

GSCs were derived from neurosurgical biopsies of human glioblastoma (TG1, TG1N, TG10 and TG16) or of grade III oligoastrocytoma (OB1), and their stem-like and tumor-initiating properties characterized as previously reported [7, 23–27]. NSCs (NSC24 and NSC25) were derived from human fetal brains, and characterized as previously described [5]. GSCs and NSCs were cultured under the form of floating cellular spheres as previously described [5, 25]. Additional cells used in this study corresponded to TG1-miR-302-367. TG1-miR-302-367 cells express in a stable manner the micro-

RNA cluster miR-302-367, previously shown to suppress the stem and tumor properties of GSCs. They were derived from TG1 as previously described [7].

### Chemicals and Antibodies

Resveratrol, sirtinol (SIRT1 and SIRT2 inhibitor), EX527 (selective SIRT1 inhibitor), AGK2 (selective SIRT2 inhibitor) and AGK7 (inactive structural isomer of AGK2) were purchased from Sigma (France). N-benzyloxycarbonyl-Val-Ala-Asp-fluoromethylketone (zVAD-fmk) was purchased from Calbiochem (San Diego, CA). All compounds were dissolved in dimethyl sulfoxide (DMSO, Sigma), according to manufacturer's instructions. The percentage of DMSO added to the cultures was at most inferior to 0.1 % and was without effect on each cell type used in this study.

Primary antibodies against the following proteins were used: LC3 (1:1000), caspase-3 (1:200) and cleaved caspase-3 (1:200) (Cell Signaling, France), SIRT1 (1:1000), SIRT2 (1:500), SIRT3 (1:500), acetylated  $\alpha$ -tubulin (1:10,000) (Santa Cruz Biotechnologies, France),  $\alpha$ -tubulin (1:50000, Millipore, France) and GAPDH (1:100,000, Chemicon International, France).

### Cell Treatments

Cells were exposed to resveratrol (50, 100, 150, 200, 250 and 300  $\mu$ M) for 24 h. Sirtuin inhibitors were used at 0.1  $\mu$ M, and added 24 h prior resveratrol treatment. zVAD-fmk was used at 100  $\mu$ M and added 30 min prior resveratrol treatment.

### Cell Proliferation, Viability and Metabolic Activity

Cell proliferation and viability were evaluated with manual cell counting under phase contrast microscopy following addition of trypan blue (Sigma) at a final concentration of 0.1 % (v/v). Cell proliferation index is equal to: Cell numbers at  $t_{24h}$ /Cell numbers at  $t_{0h}$ . Cells were seeded in 96-well plates at  $2.10^4$  cells/well, cultured for 24 h, prior to be treated with the appropriate compounds. Each treatment was assayed in quadruplet. Cell metabolic activity was assessed via measure of NAD(P)H production using reduction of WST-1 (4-[3-(4-iodophenyl)-2-(4-nitrophenyl)-2H-5-tetrazolio]-1,3-benzene disulfonate, Roche, France) to water-soluble formazan. At the end of the culture period, 10 % (v:v) WST-1 was added to the culture media, and the cells were further cultured at 37 °C for 3 h. The absorbance was measured at 430 nm in a microplate reader (Expert Plus V1.4 ASYS).

### Flow Cytometry Analysis

For cell death analysis, cells were collected, stained with Propidium Iodide (PI, 50  $\mu$ g/ml, 10 min at 4 °C, BD Biosciences,

France) then analyzed. For cell cycle analysis, cells were incubated with EdU (5-ethynyl-2'-deoxyuridine, 10  $\mu$ M, Invitrogen) for 24 h, then collected, washed in PBS, fixed with paraformaldehyde (according to manufacturer's protocol) and analyzed after PI staining. Analysis was performed on 10,000-gated events using an ARIA II (BD Biosciences, France). Blue laser (488 nm) and PE-Texas Red filter were used for PI detection, and Red laser (640 nm) and APC filter for EdU detection. Data analysis and figure generation were performed using the FACSDiva version 6.1.2 program (BD Biosciences, France).

#### Fluorescence Microscopy

Cells were cultured in EdU-containing medium (10  $\mu$ M) for 24 h, and then collected, washed in PBS, spread on glass slides, and fixed with methanol. Nuclei were stained with DAPI (200  $\mu$ g/ml, Sigma, France). Images were captured with digital still camera (DXM 1200, Nikon, USA) using Lucia software (Laboratory Imaging, Ltd). EdU fluorescence was visualized by excitation at 530–545 nm and emission at 620–660 nm (Texas Red filter). DAPI fluorescence was visualized by excitation at 340–380 nm and emission at 435–485 nm. For analysis all images were viewed and captured at 60 $\times$  magnification using an oil immersion objective. Triplicate fields were randomly selected for each slide.

#### Immunoblotting

Cells were harvested, washed with PBS, and lysed using lysis buffer (1 % SDS, 25 mM Tris-HCl pH 6.8, 0.5 mM EDTA, 0.5 mM EGTA, 1 mM sodium orthovanadate, 5 mg/ml leupeptine, 5 mg/ml pepstatin, 5 mg/ml aprotinin, 1 mM PMSF, all from Sigma). Cell lysis was performed on ice for 30 min. Proteins were resolved by 4–12 % SDS-PAGE and transferred to nitrocellulose membranes for 90 min at 15 V. The membranes were blocked with 5 % non-fat dry milk, then immunoblotted with the appropriate primary antibody overnight at 4  $^{\circ}$ C. The immune complexes were visualized using a chemiluminescent ECL detection kit (PerkinElmer, France).

#### ATP Measurement

Total ATP levels were monitored using a CellTiter-Glo Luminescent Cell Viability Assay according to the manufacturer's instructions (Promega, France). CellTiter-Glo was added to  $2.10^4$  cells/well and then placed on an orbital shaker to induce cell lysis. Luminescence was determined using an EnVision luminescence plate reader (PerkinElmer, France). Background absorbance corresponded to luminescence values of culture media containing vehicle or compound. Results are presented as percentages of the control values obtained from vehicle-treated cells.

#### Transmission Electron Microscopy

Treated cells were collected, washed in PBS, fixed in 1.6 % glutaraldehyde for 12 h at 4  $^{\circ}$ C, post fixed in 1 % osmium tetroxide (OsO<sub>4</sub>) for 1 h at room temperature, then serially dehydrated with ethanol. For transmission electron microscopy (TEM), ultrathin sections were cut on a Leica Ultra-CUT (Ultra-Microtome, Leica), stained with uranium acetate and lead citrate, then observed and photographed on a ZEISS 912 Omega TEM operating at 80 kV.

#### siRNA Transfection

Cells were transfected by electroporation using the AMAXA nucleofector device with the X005 program, and L transfection solution (LONZA, France). Anti-LC3 siRNA (siRNA LC3-A and siRNA LC3-B, 100 nM/10<sup>6</sup> cells) were kindly provided by P. Auberger, (INSERM U895, Cell death differentiation and cancer team, Nice, France). Anti-SIRT2 siRNA (300 nM/10<sup>6</sup> cells) were from Ambion (<sup>®</sup> AM16708, France). Scrambled siRNA from Ambion (<sup>®</sup> AM4611, France) was used as control. 48 h after transfection, cells were collected, lysed and assayed for protein expression by immunoblotting.

#### Statistical Analysis

Statistical analyses were done using ANOVA followed by Newman-Keuls test. A *p*-value < 0.05 was considered significant. All experiments were repeated at least thrice in an independent manner.

## Results

### Dual Dose-Dependent Inhibition of Resveratrol on GSC Proliferation and Survival

GSC exposure to 0–300  $\mu$ M of resveratrol for 24 h resulted in decreased numbers of viable cells in a dose-dependent fashion, with IC<sub>50</sub> values in the range of 150–200  $\mu$ M, as determined using the trypan blue exclusion assay (Fig. 1a). However, only GSCs treated with resveratrol concentrations above 150  $\mu$ M exhibited altered cell morphologies evoking cell death as observed under phase contrast microscopy (Fig. 1b). These results suggested that resveratrol did not induce GSC death at concentrations below 150  $\mu$ M. To evaluate cell death we performed FACS analysis on GSCs treated either with 100 or 300  $\mu$ M resveratrol. FACS analysis showed that the vast majority of GSCs underwent cell death in response to 300  $\mu$ M of resveratrol (Fig. 1c). On the opposite, 100  $\mu$ M resveratrol did not induce GSC death (Fig. 1c). Of note, metabolic activity via NAD(P)H production measured using reduction of WST-1 was robustly decreased in GSCs exposed to either 100 or

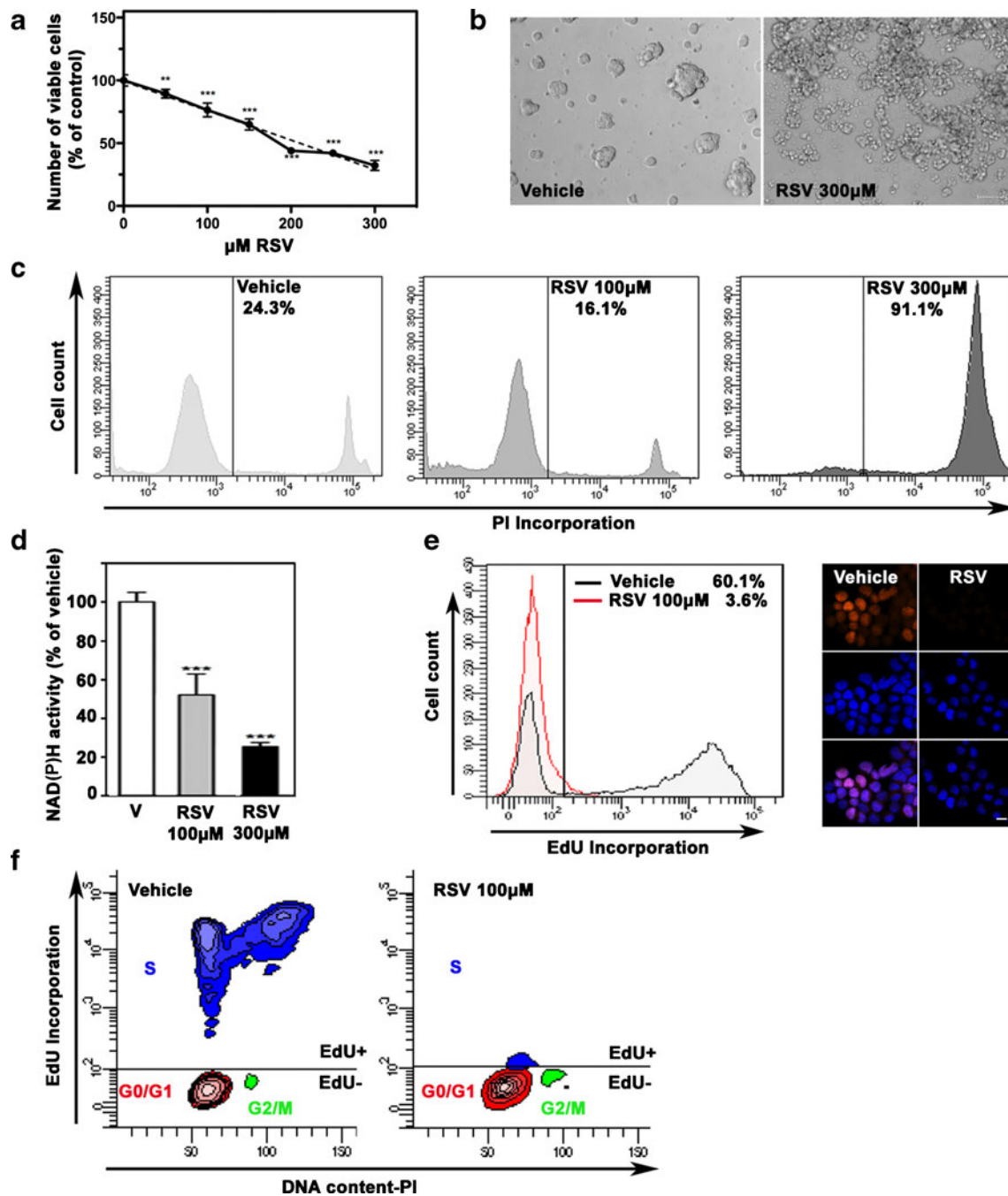


**Fig. 1** Dual dose-dependent inhibition of resveratrol on GSC proliferation and survival. **a** Dose-dependent decrease in viable GSC number induced by resveratrol (RSV 0–300  $\mu\text{M}$ , 24 h). Trypan blue exclusion assay, example of TG1 GSCs (mean  $\pm$  SD,  $n=3$ ,  $**p<0.01$ ,  $***p<0.001$ , as compared with vehicle). **b** 300  $\mu\text{M}$  resveratrol induces GSC morphological changes evoking cell death. Phase contrast microphotographs, OB1 GSCs. Bar=50  $\mu\text{M}$ . **c** Resveratrol induces GSC death only at 300  $\mu\text{M}$ . FACS analysis of propidium iodide (PI) incorporation, OB1

GSCs. **d** Resveratrol inhibits GSC metabolic activity at both 100 and 300  $\mu\text{M}$ , as shown with NAD(P)H activity assay (mean  $\pm$  SD,  $n=3$ ,  $***p<0.001$  compared with vehicle (V)). **e** 100  $\mu\text{M}$  resveratrol blocks GSC cell cycle. EdU incorporation in S-phase synthesis of the cell cycle was analyzed by FACS (left panel) and fluorescence microscopy (right panel, red signal EdU, blue DAPI). Bar=10  $\mu\text{m}$ . **f** GSC cell cycle changes induced by 100  $\mu\text{M}$  resveratrol, as shown by FACS analysis. RSV: resveratrol

300  $\mu\text{M}$  resveratrol (Fig. 1d). Altogether, these results suggested that 100  $\mu\text{M}$  resveratrol altered GSC proliferation. GSC cell cycle was therefore analyzed after incubation of the cells for 24 h with the thymidine substitute EdU (10  $\mu\text{M}$ ), which is

incorporated into newly synthesized DNA. FACS analysis showed that 100  $\mu\text{M}$  resveratrol exerted a robust inhibition of GSC proliferation, the numbers of cells having incorporated EdU being reduced  $5.6\pm 1.9$  fold (mean  $\pm$  SD,  $n=4$ ) (Fig. 1e).

Refined cell cycle analysis using EdU to label cells having undergone DNA replication, and PI as an index of DNA content, showed that in presence of 100  $\mu$ M resveratrol, GSCs accumulate in the G0/G1 phase with a concomitant depletion of cells in the S phase (52–57 % cells in S phase in control condition versus 7–9 % cells in resveratrol-treated cultures) (Fig. 1f).

### Resveratrol Inhibits GSC Proliferation and Survival but Sparing Normal NSCs

Resveratrol has been repetitively reported to be either innocuous or beneficial for normal non-cancerous neural cells but its effects on normal human NSCs remain unexplored. We therefore compared the proliferation and survival of five GSC cultures (OB1, TG1, TG1N, TG10 and TG16) with those of human NSCs following exposure to 100  $\mu$ M and 300  $\mu$ M resveratrol. Resveratrol did not modify the proliferation and viability of human NSCs (Fig. 2a and b, respectively) nor their morphology (data not shown). On the opposite, and as expected, resveratrol inhibited the proliferation of all GSC cultures at 100  $\mu$ M (Fig. 2a), and triggered severe GSC death at 300  $\mu$ M (Fig. 2b). Of note, resveratrol effects on GSCs were independent from the transcription factor p53, a well-known regulator of cell survival. Resveratrol effects were observed in GSCs bearing either a wild type (OB1, TG1, TG1N), or a mutant form of *TP53* (TG10, TG16) [23] (Fig. 2a and b).

Finally, we verified whether resveratrol could act on GSCs once they have been induced to lose their stem and tumor-initiating properties. For this purpose, we used GSCs cultured in serum-supplemented medium, which is known to result in loss of stem-like and tumorigenic properties [23, 28]. We also explored resveratrol effects on GSCs transduced with the cluster of microRNAs, miR-302-367 that commits GSCs to an irreversible non stem-like state, and suppress their ability to initiate tumors [7]. Our results showed that the proliferation and the survival of GSCs having lost their properties were also inhibited in presence of 100 or 300  $\mu$ M resveratrol, respectively (Fig. 2c and d).

100  $\mu$ M resveratrol inducing only cell cycle blockade without altering GSC survival, we envisaged the possibility that autophagy could protect the cells against cell death, as previously reported in other types of cancer cells [29, 30]. We used LC3-II expression as a marker of autophagy, a cell process allowing the degradation of superfluous or damaged proteins and organelles through the formation of autophagolysosomes. LC3-II results from the processing of LC3-I and is required for the formation of autophagolysosomes [31]. Western blot analysis with an antibody recognizing both forms of the protein, revealed an up-regulation of LC3-II in resveratrol-treated cells (Fig. 3a). Resveratrol did not induce LC3-II expression in NSCs (Fig. 3a). Presence of autophagosomes/autophagolysosomes was observed using transmission electron microscopy of GSCs treated with 100  $\mu$ M resveratrol

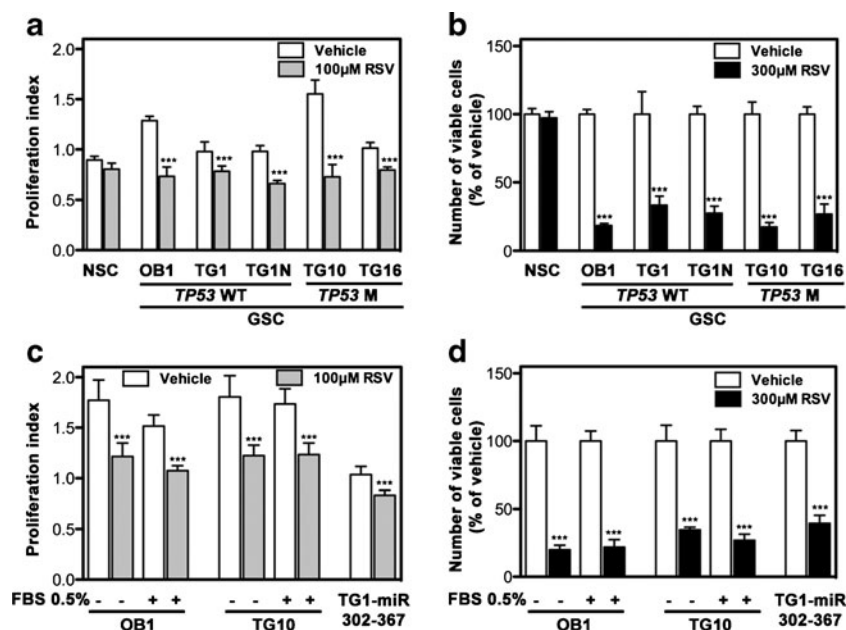


**Fig. 2** Resveratrol inhibits GSC proliferation and survival whereas sparing NSCs. **a and b** Comparative effects of resveratrol on NSC and GSC proliferation (**a**) and survival (**b**). Viable cell numbers were determined using trypan blue exclusion assay. Note that all GSCs tested were sensitive to the inhibitory effects of resveratrol regardless of the presence of a wild-type (WT) or mutant (M) form of *TP53* (mean  $\pm$  SD,  $n=3$ ,

\*\*\* $p<0.001$  as compared with the respective vehicle condition). **c and d** Resveratrol inhibits the proliferation (**c**) and survival (**d**) of GSCs having lost their stem properties, either in response to serum (FBS) treatment, or to viral transduction of the micro-RNA cluster miR-302-367 (mean  $\pm$  SD,  $n=3$ , \*\*\* $p<0.001$  as compared with the respective vehicle condition). See text for further details

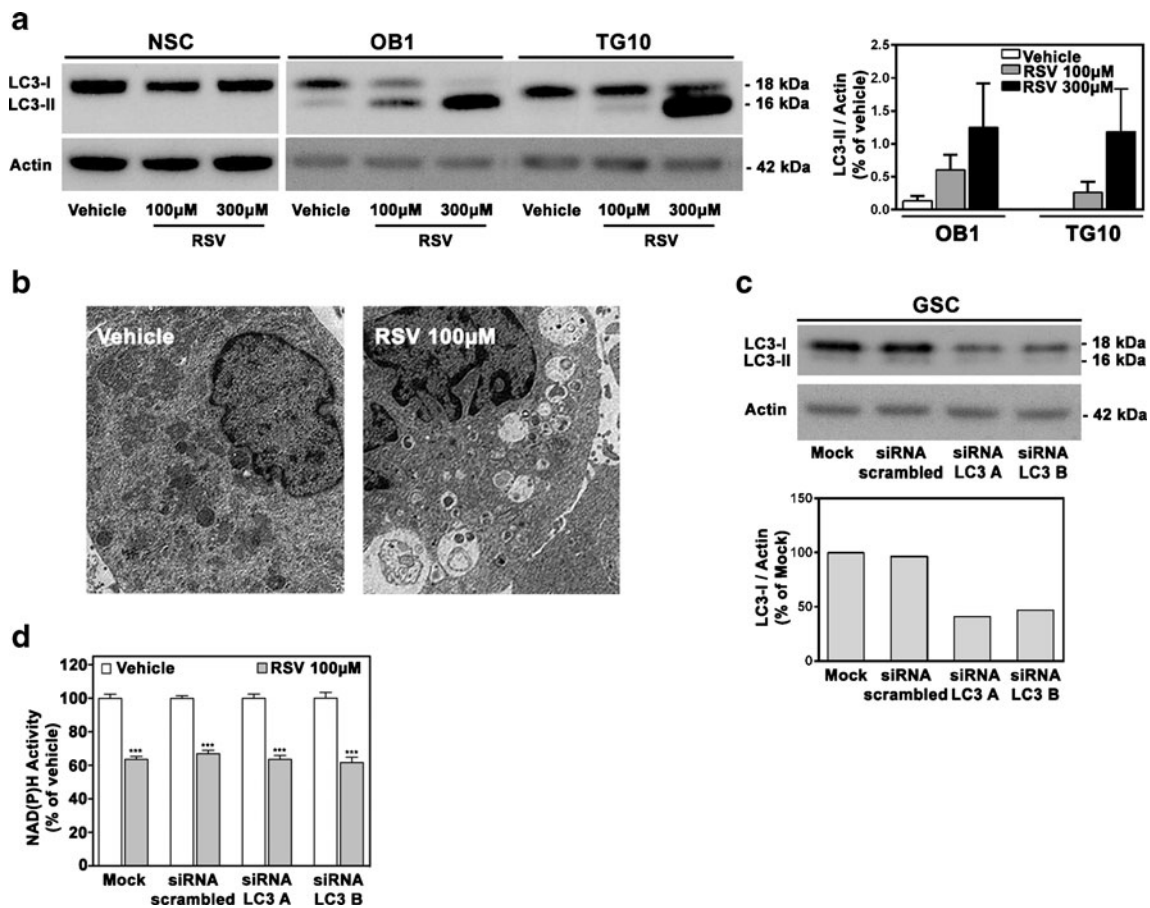


**Fig. 3** Resveratrol induces autophagy in GSCs. **a** Resveratrol induces LC3-II formation in GSCs but not in NSCs. *Left panel*: total cell lysates from NSCs and GSCs were analyzed for LC3-I and LC3-II expression by immunoblotting. Actin was used as a loading control. *Right panel*: densitometric analysis of LC3-II immunoreactive signals (mean  $\pm$  SD,  $n=3$ ). **b** Autophagosomes were observed by transmission electronic microscopy in GSCs treated with 100  $\mu$ M resveratrol. **c** Decreased

protein expression of LC3 in GSCs transfected with anti-LC3 siRNAs, as compared to mock-transfected GSCs or to GSCs transfected with scrambled siRNA (*top panel*) and densitometric analysis of LC3 immunoreactive signal (*bottom panel*). **d** Down-regulated expression of LC3 does not modify resveratrol inhibitory effect on metabolic activity. NAD(P)H activity assay (mean  $\pm$  SD,  $n=3$ ,  $***p<0.001$  as compared with the respective vehicle condition)

(Fig. 3b). Inhibition of LC3 expression with siRNA transfection (Fig. 3c) did not modify GSC response to either 100  $\mu$ M (Fig. 3d) or 300  $\mu$ M resveratrol (not shown). These results indicate that autophagy does not interfere with resveratrol action on GSCs.

#### SIRT2 Participates in Resveratrol-Induced Cell Cycle Inhibition

To explore the mechanisms underlying resveratrol effects, we focused our attention on the family of NAD-dependent deacetylases sirtuins, one of its members SIRT1 having been repetitively shown to constitute a preferential resveratrol target at least in normal cells [32]. Western blot analysis showed that SIRT1 and SIRT3 were expressed by both GSCs and NSCs whereas SIRT2 expression was restricted to GSCs (Fig. 4a). This observation suggested a role for SIRT2 in mediating resveratrol effects in GSCs. We first tested this hypothesis using pharmacological inhibitors of sirtuins. Sirtinol, a non-

selective sirtuin inhibitor targeting both SIRT1 and SIRT2, reverted the inhibition of GSC proliferation induced by resveratrol (Fig. 4b). EX527, a specific inhibitor of SIRT1 activity, failed to restore GSC proliferation (Fig. 4b). On the opposite, the specific SIRT2 inhibitor AGK2 prevented the inhibitory effect of resveratrol on GSC proliferation, whereas its inactive isomer AGK7 had no effect (Fig. 4b). All SIRT inhibitors failed to restore resveratrol-induced cell death (Fig. 4c). To further assay the involvement of SIRT2 in resveratrol-induced inhibition of GSC proliferation, we down-regulated SIRT2 expression using specific siRNAs. SIRT2 protein levels were reduced 2.7 fold in GSCs transfected with SIRT2 siRNAs, as compared to GSCs transfected with scrambled siRNAs (Fig. 4d). Analysis of cell proliferation by cell counting showed that inhibition of SIRT2 expression decreased by half the deleterious effect of resveratrol on GSC proliferation (Fig. 4e). The targeting of SIRT2 by resveratrol was further verified by examination of the

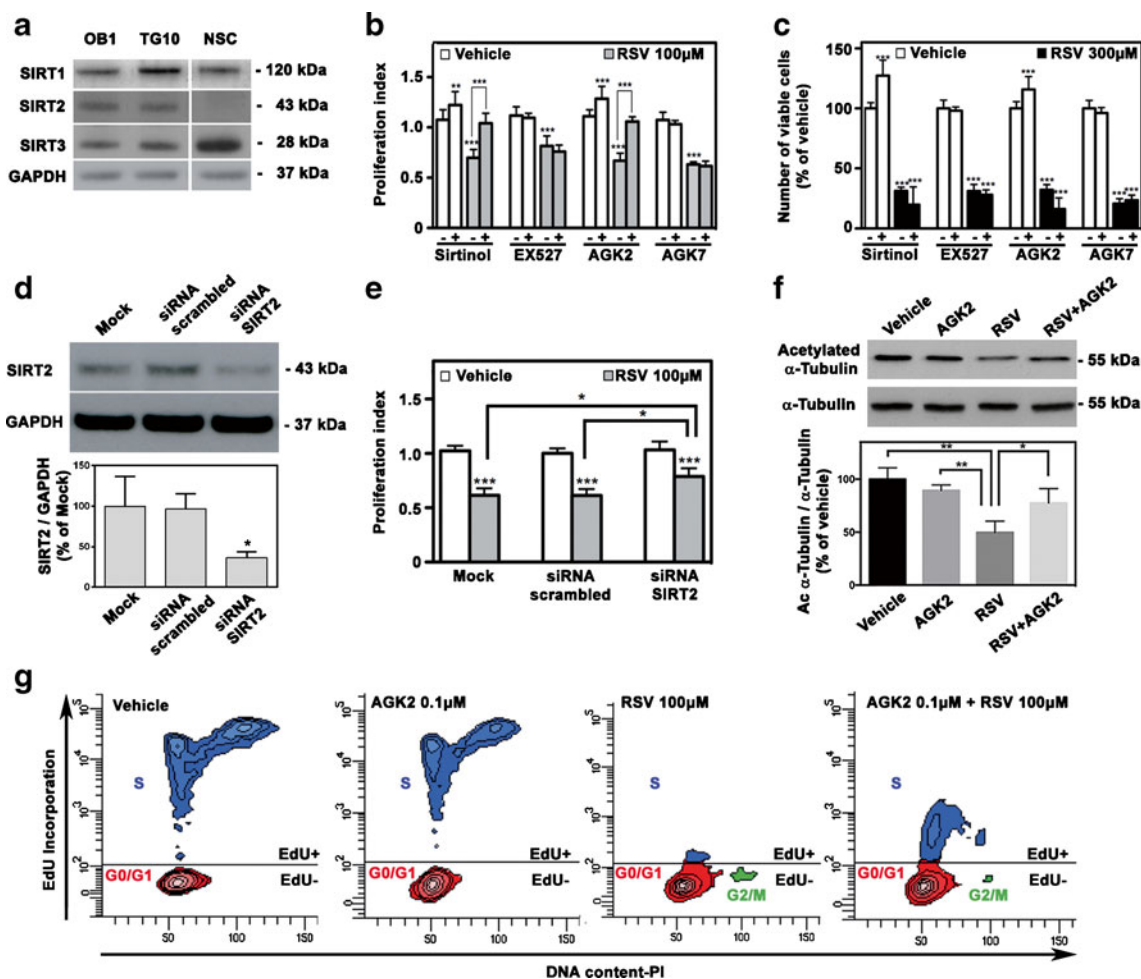


**Fig. 4** Resveratrol-induced GSC cell cycle arrest depends on SIRT2. **a** Total cell lysates from NSCs and GSCs were analyzed for SIRT1, SIRT2 and SIRT3 expression by immunoblotting. GAPDH was used as a loading control. Note that NSCs do not express SIRT2. **b** Pharmacological inhibition of SIRT2 counteracts the inhibitory effects exerted by 100  $\mu$ M resveratrol on GSC proliferation (mean  $\pm$  SD,  $n=3$ , \*\* $p<0.01$ , \*\*\* $p<0.001$ ). Statistical significance, as compared to the vehicle condition—is shown with stars on top of the bars. Statistical significance, as compared to resveratrol-treated cells with no inhibitor is shown with stars on top of the lines joining the bars. **c** Resveratrol-induced GSC death is maintained in presence of sirtuin inhibitors (mean  $\pm$  SD,  $n=3$ , \*\*\* $p<0.001$ , as compared to the respective vehicle condition). **d** Decreased expression of SIRT2 protein in GSCs transfected with anti-SIRT2 siRNA, as compared to mock transfected

GSCs or to GSCs transfected with scrambled siRNA. *Bottom panel:* densitometric analysis (mean  $\pm$  SD,  $n=3$ , \* $p<0.05$  as compared with mock-transfected GSCs or GSCs transfected with scrambled siRNA). **e** Down-regulated expression of SIRT2 counteracts resveratrol inhibitory effects on GSC proliferation (mean  $\pm$  SD,  $n=3$ , \* $p<0.05$ , \*\*\* $p<0.001$ ). Representation of the statistical comparisons as in **b**. **f** Resveratrol promotes the deacetylation of  $\alpha$ -tubulin, a substrate of SIRT2. *Bottom panel:* densitometric analysis (mean  $\pm$  SD,  $n=3$ , \* $p<0.05$ , \*\* $p<0.01$ ). **g** Blockade of SIRT2 activity with AGK2 prevents resveratrol-induced GSC cell cycle arrest. Cell cycle profile was analyzed by FACS on GSCs exposed to EdU prior to be fixed and labeled with propidium iodide (PI). In **b**, **c** and **e**, viable cell numbers were determined using trypan blue exclusion assay

acetylation levels of  $\alpha$ -tubulin, a SIRT2 substrate [33]. Immunoblotting with antibodies recognizing either all forms of  $\alpha$ -tubulin or its acetylated form (acetylated K40) showed that resveratrol treatment resulted in decreased levels of acetylated- $\alpha$ -tubulin, and AGK2 prevented resveratrol-induced  $\alpha$ -tubulin deacetylation (Fig. 4f). Finally, we evaluated whether blockade of SIRT2 activity with AGK2 prevented resveratrol-induced cell cycle arrest of GSCs using EdU and PI incorporation followed by FACS analysis. AGK2 was without effect on the cell cycle of vehicle-treated cells. On the opposite, treatment of GSCs with

AGK2 reduced the inhibition of cell cycle progression in resveratrol-treated GSCs, increasing the numbers of cells in S phase from 1.4 to 2 fold (Fig. 4g).

#### Resveratrol Induces GSC Necrosis by a SIRT2 Independent Mechanism

To determine the type of cell death underwent by GSCs treated with 300  $\mu$ M resveratrol, we first evaluated a possible involvement of apoptosis, a mode of death requiring stable

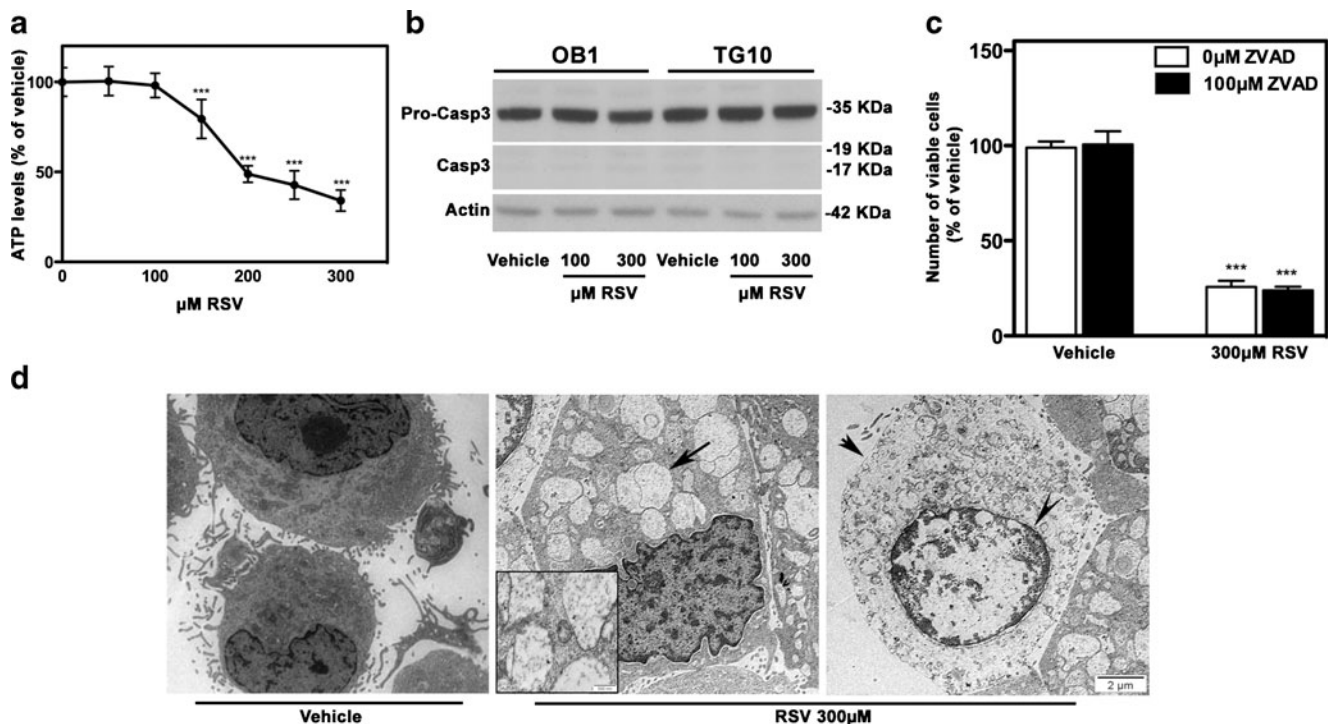


**Fig. 5** 300 μM resveratrol induces GSC necrosis. **a** Resveratrol inhibits GSC ATP production in a dose-dependent manner ( $n=3$ ,  $***p<0.001$  as compared with vehicle condition). **b** Resveratrol does not induce caspase-3 activation. Illustration of 3 independent experiments. **c** The pan-caspase inhibitor zVAD-fmk (ZVAD) does not prevent resveratrol-induced GSC death. GSCs were treated for 30 min with ZVAD (100 μM) prior additional exposure to resveratrol for 24 h. Viable cell numbers were

determined using trypan blue exclusion assay ( $n=3$ ,  $***p<0.001$ , as compared with the respective vehicle condition). **d** Electronic microscopy images illustrating GSC morphological changes following 24 h exposure to 300 μM resveratrol. Note the swelling of organelles (arrow) and fragmentation of nuclear and cell membrane (short arrow and arrowheads, respectively). Bar=2 μm and 500 nm in insert

ATP concentrations and caspase activation [34], regardless of the specific sub-apoptotic pathway used by the cell. Accordingly, we measured ATP production and observed a robust ATP depletion in GSCs only within the 200–300 μM resveratrol concentration range (Fig. 5a), as expected for a mode of death independent from apoptosis. We then sought for caspase mobilization that governs subsequent signaling cascades ending up in cell apoptosis. We first focused on caspase-3, this caspase being the most frequently shown to be activated during apoptosis, regardless of the cell type and the apoptosis-inducing signal considered. The results showing unchanged levels of activated caspase-3 (Fig. 5b), we used the broad-spectrum pan-caspase inhibitor zVAD-fmk to verify whether other caspases could be involved in resveratrol-induced cell death. This pan-caspase inhibitor did not provide any protection against resveratrol-induced GSC death (Fig. 5c). Altogether, these results show that resveratrol does not trigger GSC apoptosis. Characterization of the morphology of 300 μM resveratrol-treated cells by transmission electron microscopy showed numerous morphological changes including grossly swollen organelles, and fragmentation of the nuclear and cell membranes (Fig. 5d). These morphological alterations, associated with the drop in ATP levels characteristic of cell necrosis [34] indicate, that GSCs undergo necrosis in response to 300 μM resveratrol.

## Discussion

The results of this study show that resveratrol exerts a dual effect on glioblastoma cells endowed with stem-like properties, inhibiting cell cycling at doses lesser than 150 μM and triggering necrosis above 150 μM, whereas sparing normal human NSCs. Pharmacological inhibition of SIRT2 with the AGK2 compound, and down-regulated SIRT2 expression with siRNAs disclose a role for SIRT2 activity as a mediator of the inhibitory action of resveratrol on GSC cell cycle. On the opposite, GSC necrosis induced by higher doses of resveratrol is independent from sirtuin activity.

Previous studies on the adverse effects of resveratrol on cancer cell growth have disclosed interactions with multiple molecular targets in several different cancer cells of hematological, epithelial and central nervous system origins [35, 36]. Accordingly, resveratrol exerts varied actions on cancer cell behavior that range from cell cycle disruption to induction of apoptosis or necrosis [17, 37–40]. Similarly to the GSCs studied in the present work, the U87 and U251 glioma cell lines have been reported to respond to 100–300 μM resveratrol with cell cycle arrest, and induction of autophagy. However, the role of autophagy differs between GSCs and these classic glioma cell lines. Cell cycle arrest in resveratrol-treated



U87 and U251 cells depends on the induction of autophagy, the induction of which concomitantly prevents resveratrol-induced apoptosis [17, 41]. In GSCs, down-regulated expression of the key component of autophagolysosomes LC3 did not modify GSC response to resveratrol. Resveratrol (50–200  $\mu\text{M}$ ) was recently reported to sensitize GSCs to irradiation-induced death [42]. This effect was correlated with an inhibition of STAT3 signaling in the presence of resveratrol, STAT3 being known for its involvement in the maintenance of GSC properties. In this study using CD133+ GSCs, resveratrol did not affect LC3-II levels, the high LC3-II levels already present in control conditions suggesting the existence of a metabolic stress, as expected in CD133 expressing cells [43]. Additional differences in cell contexts could account for variations in resveratrol actions, such as different abilities in resveratrol biotransformation, especially through its metabolism in sulfate and glucuronide conjugates [18, 38, 44]. They could also differ in the expression of ABC transporters, xenobiotic protectors known to constrain resveratrol bioavailability [45], and highly active in the GSCs used in the present study (team Glial Plasticity, unpublished results). Although further studies are required to pinpoint the source of these variable responses of GSCs to resveratrol, these results suggest that resveratrol acts in a variety of manners and mechanisms on GSCs as it does on classic glioma cell lines. All these pleiotropic actions limit tumor progression. Resveratrol was reported to induce U251 cell apoptosis with inhibition of the pro-survival PI3K/Akt/mTOR transduction pathway [19]. Study of T98G and A172 glioma cells, which bear a heterozygous *TP53* mutation, has shown an alternative mechanism of action. In these cells, resveratrol induces apoptosis by restoring a Notch1-p53 signaling pathway [20]. The present results show that resveratrol can inhibit cell cycle and survival of GSCs bearing distinct genomic alterations [23, 25] (mutant or wild-type *TP53* and/or mutant or wild-type *PTEN*, a tumor suppressing gene which regulates the activity of the PI3K/Akt pathway known to be essential for GSC survival) [26, 46]. However, resveratrol effects appearing to critically depend on the whole metabolic capacity of the cell under scrutiny, as well as on the set of target proteins expressed by the cells, we cannot exclude the possibility that additional resveratrol targets are expressed in the GSCs used in this study.

Our results additionally showed that survival inhibition of GSCs induced by 300  $\mu\text{M}$  resveratrol occurs through necrosis rather than apoptosis, as previously described for C6 rat glioma cell line [38]. Contrary to apoptosis, necrosis is an energy-independent death process characterized by loss of membrane integrity, cell swelling and ultimately cell lysis. GSCs exposed to 300  $\mu\text{M}$  resveratrol exhibited all characteristics of necrosis with ATP depletion, organelle and cell swelling, and membrane disruption [34, 47]. We did not observe any of the characteristics of apoptosis, including cytoplasmic shrinking, nuclear condensation (as shown by electronic microscopy), or

caspace activation (as shown by the lack of cell rescue with the pan-caspase inhibitor ZVAD or caspase-3 immunoblotting).

Necrosis is predominantly viewed as a passive, unorganized death pathway [48], although some forms of programmed necrosis have been reported. A very recent report has noteworthy placed SIRT2 at the core of programmed necrosis [14]. In GSCs, blockade of SIRT2 expression or enzymatic activity did not counteract resveratrol-induced necrosis, suggesting that in that case necrosis is likely the result of a disordered catastrophic response of the cells to severe energy depletion. On the opposite, our results show that SIRT2 mediates resveratrol inhibitory effect on GSC cell cycle. They are coherent with previous reports of resveratrol effect on human SIRT2 in vitro. Using recombinant hSIRT2 or the inactive mutant hSIRT2N168A, and  $\alpha$ -tubulin as a substrate, Suzuki et al. [49] have shown that 100  $\mu\text{M}$  resveratrol robustly stimulated hSIRT2 activity. Likewise, Fan et al. [50], using recombinant SIRT2 and Fmoc-labeled peptides as substrates reported SIRT2 activation with 100  $\mu\text{M}$  resveratrol. Regarding sirtuin pharmacological inhibitors, Outeiro et al. [51] have reported that AGK2 inhibits recombinant SIRT2 activity in vitro with an IC<sub>50</sub> of 3.5  $\mu\text{M}$ , whereas only 0.2  $\mu\text{M}$  AGK2 are required to fully reverse the SIRT2-dependent deleterious effect of mutated  $\alpha$ -synuclein expression in dopaminergic neurons. Post-translational modifications of SIRT2, and/or co-factors are likely to underlie the differences observed in AGK2 efficiency, but the precise molecular mechanism remains to be elucidated.

Either down-regulated expression of SIRT2 or pharmacological blockade of its enzymatic activity counteracted resveratrol-induced cell cycle arrest. The results of the present study are in accordance with the reported correlation between SIRT2 expression with cell cycle progression, and the peak of SIRT2 expression observed during mitosis [52]. Altogether, our results show that resveratrol can target members of the sirtuin family in GSCs, as in normal neural cells [53, 54]. With respect to NSCs, we did not observe any positive or negative change in cell behavior following resveratrol treatment, although these cells had high protein levels of at least two members of the sirtuin family, SIRT1 and SIRT3. This observation is in accordance with the lack of effect of resveratrol on wild-type murine NSCs [55]. On the opposite, resveratrol prevents depletion in NSC numbers in mice deficient for the metalloprotease Zmpste24 responsible for prelamin A maturation, a model of the syndrome of premature aging, progeria [55]. In mutant NSCs, resveratrol restores SIRT1 association with nuclear matrix, and hence its enzymatic activity, both decreased in the presence of prelamin A. Sirtuins have received numerous credits as supporting the beneficial effects of resveratrol in normal cells whereas their involvement in resveratrol deleterious effect on transformed cells was the matter of only a single report where inhibition of their proliferation was associated with SIRT1-dependent AMPK activation [56]. We now provide a second example for the involvement of a

sirtuin, namely SIRT2, in a deleterious effect of resveratrol on cancerous cells, here on GSCs. These data of the literature, associated with the present results suggest that the type of response of a given cell to resveratrol does not merely rely on the presence or absence of a given protein, but rather on the existence of complex protein interactions that remain to be identified. They further stretch out the importance of the cell context in determining the outcome of resveratrol effects.

**Acknowledgments** The authors thank Amélia Dias-Morais for excellent technical assistance, and are grateful to Dr P. Auberger (INSERM U895, Nice, France) for providing LC3 siRNA. This work was supported by ARC and by Région Ile de France-Canceropôle (CT and EAE fellowships), and by CAPES/COFECUB (LGD and AB fellowships).

**Conflict of Interest** The authors declare no conflict of interest.

## References

- Stupp, R., Mason, W. P., van den Bent, M. J., et al. (2005). Radiotherapy plus concomitant and adjuvant temozolomide for glioblastoma. *The New England Journal of Medicine*, *352*(10), 987–996.
- Bao, S., Wu, Q., McLendon, R. E., et al. (2006). Glioma stem cells promote radioresistance by preferential activation of the DNA damage response. *Nature*, *444*(7120), 756–760.
- Diehn, M., & Clarke, M. F. (2006). Cancer stem cells and radiotherapy: new insights into tumor radioresistance. *Journal of the National Cancer Institute*, *98*(24), 1755–1757.
- Chen, J., Li, Y., Yu, T. S., et al. (2012). A restricted cell population propagates glioblastoma growth after chemotherapy. *Nature*, *488*(7412), 522–526.
- Thirant, C., Bessette, B., Varlet, P., et al. (2011). Clinical relevance of tumor cells with stem-like properties in pediatric brain tumors. *PLoS ONE*, *6*(1), e16375.
- Zbinden, M., Duquet, A., Lorente-Trigos, A., et al. (2010). NANOG regulates glioma stem cells and is essential in vivo acting in a cross-functional network with GLI1 and p53. *The EMBO Journal*, *29*(15), 2659–2674.
- Fareh, M., Turchi, L., Virolle, V., et al. (2012). The miR 302–367 cluster drastically affects self-renewal and infiltration properties of glioma-initiating cells through CXCR4 repression and consequent disruption of the SHH-GLI-NANOG network. *Cell death and differentiation*, *19*(2), 232–244.
- Eyler, C. E., & Rich, J. N. (2008). Survival of the fittest: cancer stem cells in therapeutic resistance and angiogenesis. *Journal of Clinical Oncology*, *26*(17), 2839–2845.
- Aggarwal, B. B., Bhardwaj, A., Aggarwal, R. S., Seeram, N. P., Shishodia, S., & Takada, Y. (2004). Role of resveratrol in prevention and therapy of cancer: preclinical and clinical studies. *Anticancer Research*, *24*(5A), 2783–2840.
- Narita, K., Hisamoto, M., Okuda, T., & Takeda, S. (2011). Differential neuroprotective activity of two different grape seed extracts. *PLoS ONE*, *6*(1), e14575.
- Sun, A. Y., Wang, Q., Simonyi, A., & Sun, G. Y. (2010). Resveratrol as a therapeutic agent for neurodegenerative diseases. *Molecular Neurobiology*, *41*(2–3), 375–383.
- Milne, J. C., Lambert, P. D., Schenk, S., et al. (2007). Small molecule activators of SIRT1 as therapeutics for the treatment of type 2 diabetes. *Nature*, *450*(7170), 712–716.
- Vaziri, H., Dessain, S. K., NgEaton, E., et al. (2001). hSIR2(SIRT1) functions as an NAD-dependent p53 deacetylase. *Cell*, *107*(2), 149–159.
- Narayan, N., Lee, I. H., Borenstein, R., et al. (2012). The NAD-dependent deacetylase SIRT2 is required for programmed necrosis. *Nature*, *492*(7428), 199–204.
- Hiratsuka, M., Inoue, T., Toda, T., et al. (2003). Proteomics-based identification of differentially expressed genes in human gliomas: down-regulation of SIRT2 gene. *Biochemical and Biophysical Research Communications*, *309*(3), 558–566.
- Zhang, W., Murao, K., Zhang, X., et al. (2010). Resveratrol represses YKL-40 expression in human gliomaU87 cells. *BMC Cancer*, *10*, 593.
- Filippi-Chiela, E. C., VillodreES, Z. L. L., & Lenz, G. (2011). Autophagy interplay with apoptosis and cell cycle regulation in the growth inhibiting effect of resveratrol in glioma cells. *PLoS ONE*, *6*(6), e20849.
- Shu, X. H., Li, H., Sun, X. X., et al. (2011). Metabolic patterns and biotransformation activities of resveratrol in human glioblastoma cells: relevance with therapeutic efficacies. *PLoS ONE*, *6*(11), e27484.
- Jiang, H., Zhang, L., Kuo, J., et al. (2005). Resveratrol-induced apoptotic death in human U251 glioma cells. *Molecular Cancer Therapeutics*, *4*(4), 554–561.
- Lin, H., Xiong, W., Zhang, X., et al. (2011). Notch-1 activation-dependent p53 restoration contributes to resveratrol-induced apoptosis in glioblastoma cells. *Oncology Reports*, *26*(4), 925–930.
- Lin, C. J., Lee, C. C., Shih, Y. L., et al. (2012). Resveratrol enhances the therapeutic effect of temozolomide against malignant glioma in vitro and in vivo by inhibiting autophagy. *Free Radical Biology and Medicine*, *52*(2), 377–391.
- Huang, H., Lin, H., Zhang, X., & Li, J. (2012). Resveratrol reverses temozolomide resistance by downregulation of MGMT in T98G glioblastoma cells by the NF- $\kappa$ B-dependent pathway. *Oncology Reports*, *27*(6), 2050–2056.
- Silvestre, D. C., Pineda, J. R., Hoffschir, F., et al. (2011). Alternative lengthening of telomeres in human glioma stem cells. *Stem Cells*, *29*(3), 440–451.
- Surena, A. L., de Faria, G. P., Studler, J. M., et al. (2009). DLG1/SAP97 modulates transforming growth factor alpha bioavailability. *Biochimica et Biophysica Acta*, *1793*(2), 264–272.
- Patru, C., Romao, L., Varlet, P., et al. (2010). CD133, CD15/SSEA-1, CD34 or side populations do not resume tumor-initiating properties of long-term cultured cancer stem cells from human malignant glioblastoma. *BMC Cancer*, *10*, 66.
- Galan-Moya, E. M., Le Guelte, A., Lima Fernandes, E., et al. (2011). Secreted factors from brain endothelial cells maintain glioblastoma stem-like cell expansion through the mTOR pathway. *EMBO Reports*, *12*(5), 470–476.
- Thirant, C., Galan-Moya, E. M., Dubois, L. G., et al. (2012). Differential proteomic analysis of human glioblastoma and neural stem cells reveals HDGF as a novel angiogenic secreted factor. *Stem Cells*, *30*(5), 845–853.
- Lee, J., Kotliarova, S., Kotliarov, Y., et al. (2006). Tumor stem cells derived from glioblastomas cultured in bFGF and EGF more closely mirror the phenotype and genotype of primary tumors than do serum-cultured cell lines. *Cancer Cell*, *9*(5), 391–403.
- Degenhardt, K., Mathew, R., Beaudoin, B., et al. (2006). Autophagy promotes tumor cell survival and restricts necrosis, inflammation, and tumorigenesis. *Cancer Cell*, *10*(1), 51–64.
- Mathew, R., Karantza-Wadsworth, V., & White, E. (2007). Role of autophagy in cancer. *Nature Reviews. Cancer*, *7*(12), 961–967.
- Kabeya, Y., Mizushima, N., Ueno, T., et al. (2000). LC3, a mammalian homologue of yeast Apg8p, is localized in autophagosomal membranes after processing. *The EMBO Journal*, *19*(21), 5720–5728.
- Baur, J. A. (2010). Resveratrol, sirtuins, and the promise of a DR mimetic. *Mechanisms of Ageing and Development*, *131*(4), 261–269.

33. North, B. J., Marshall, B. L., Borra, M. T., Denu, J. M., & Verdin, E. (2003). The human Sir2 ortholog, SIRT2, is an NAD<sup>+</sup>-dependent tubulin deacetylase. *Molecular Cell*, *11*(2), 437–444.
34. Leist, M., Single, B., Castoldi, A. F., Kühnle, S., & Nicotera, P. (1997). Intracellular adenosine triphosphate (ATP) concentration: a switch in the decision between apoptosis and necrosis. *The Journal of Experimental Medicine*, *185*(8), 1481–1486.
35. Athar, M., Back, J. H., Tang, X., et al. (2007). Resveratrol: a review of preclinical studies for human cancer prevention. *Toxicology and Applied Pharmacology*, *224*(3), 274–283.
36. Gagliano, N., Aldini, G., Colombo, G., et al. (2010). The potential of resveratrol against human gliomas. *Anti-cancer Drugs*, *21*(2), 140–150.
37. Aziz, M. H., Nihal, M., Fu, V. X., Jarrard, D. F., & Ahmad, N. (2006). Resveratrol-caused apoptosis of human prostate carcinoma LNCaP cells is mediated via modulation of phosphatidylinositol 3'-kinase/Akt pathway and Bcl-2 family proteins. *Molecular Cancer Therapeutics*, *5*(5), 1335–1341.
38. Michels, G., Wätjen, W., Weber, N., et al. (2006). Resveratrol induces apoptotic cell death in rat H4IIE hepatoma cells but necrosis in C6 glioma cells. *Toxicology*, *225*(2–3), 173–182.
39. Vanamala, J., Reddivari, L., Radhakrishnan, S., & Tarver, C. (2010). Resveratrol suppresses IGF-1 induced human colon cancer cell proliferation and elevates apoptosis via suppression of IGF-1R/Wnt and activation of p53 signaling pathways. *BMC Cancer*, *10*, 238.
40. Puissant, A., Robert, G., Fenouille, N., et al. (2010). Resveratrol promotes autophagic cell death in chronic myelogenous leukemia cells via JNK-mediated p62/SQSTM1 expression and AMPK activation. *Cancer Research*, *70*(3), 1042–1052.
41. Li, J., Qin, Z., & Liang, Z. (2009). The prosurvival role of autophagy in Resveratrol-induced cytotoxicity in human U251 glioma cells. *BMC Cancer*, *9*, 215.
42. Yang, Y. P., Chang, Y. L., Huang, P. I., et al. (2012). Resveratrol suppresses tumorigenicity and enhances radiosensitivity in primary glioblastoma tumor initiating cells by inhibiting the STAT3 axis. *Journal of Cellular Physiology*, *227*(3), 976–993.
43. Griguer, C. E., Oliva, C. R., Gobin, E., et al. (2008). CD133 is a marker of bioenergetic stress in human glioma. *PLoS ONE*, *3*(11), e3655.
44. Wenzel, E., Soldo, T., Erbersdobler, H., & Somoza, V. (2005). Bioactivity and metabolism of trans-resveratrol orally administered to Wistar rats. *Molecular Nutrition and Food Research*, *49*(5), 482–494.
45. Planas, J. M., Alfaras, I., Colom, H., & Juan, M. E. (2012). The bioavailability and distribution of trans-resveratrol are constrained by ABC transporters. *Archives of Biochemistry and Biophysics*, *527*(2), 67–73.
46. Hambardzumyan, D., Squatrito, M., Carbajal, E., & Holland, E. C. (2008). Glioma formation, cancer stem cells, and akt signaling. *Stem Cell Reviews*, *4*(3), 203–210.
47. Kroemer, G., Galluzzi, L., Vandenabeele, P., et al. (2009). Classification of cell death: recommendations of the Nomenclature Committee on Cell Death 2009. *Cell Death and Differentiation*, *16*(1), 3–11.
48. Edinger, A. L., & Thompson, C. B. (2004). Death by design: apoptosis, necrosis and autophagy. *Current Opinion in Cell Biology*, *16*(6), 663–669.
49. Suzuki, K., & Koike, T. (2007). Resveratrol abolishes resistance to axonal degeneration in slow Wallerian degeneration (WldS) mice: activation of SIRT2, an NAD-dependent tubulin deacetylase. *Biochemical and Biophysical Research Communications*, *359*(3), 665–671.
50. Fan, Y., Ludewig, R., & Scriba, G. K. (2009). 9-Fluorenylmethoxycarbonyl-labeled peptides as substrates in a capillary electrophoresis-based assay for sirtuin enzymes. *Analytical Biochemistry*, *387*(2), 243–248.
51. Outeiro, T. F., Kontopoulos, E., Altmann, S. M., et al. (2007). Sirtuin 2 inhibitors rescue alpha-synuclein-mediated toxicity in models of Parkinson's disease. *Science*, *317*(5837), 516–519.
52. Inoue, T., Hiratsuka, M., Osaki, M., & Oshimura, M. (2007). The molecular biology of mammalian SIRT proteins: SIRT2 in cell cycle regulation. *Cell Cycle*, *6*(9), 1011–1018.
53. Anekonda, T. S. (2006). Resveratrol—a boon for treating Alzheimer's disease? *Brain Research Reviews*, *52*(2), 316–326.
54. Pfister, J. A., Ma, C., Morrison, B. E., & D'Mello, S. R. (2008). Opposing effects of sirtuins on neuronal survival: SIRT1-mediated neuroprotection is independent of its deacetylase activity. *PLoS ONE*, *3*(12), e4090.
55. Liu, B., Ghosh, S., Yang, X., et al. (2012). Resveratrol rescues SIRT1-dependent adult stem cell decline and alleviates progeroid features in laminopathy-based progeria. *Cell Metabolism*, *16*(6), 738–750.
56. Lin, J. N., Lin, V. C., Rau, K. M., et al. (2010). Resveratrol modulates tumor cell proliferation and protein translation via SIRT1-dependent AMPK activation. *Journal of Agricultural and Food Chemistry*, *58*(3), 1584–1592.